

Published in final edited form as:

Polym Chem. 2014 March 21; 5(6): 1954–1964. doi:10.1039/C3PY01338C.

Labelling Polymers and Micellar Nanoparticles via Initiation, Propagation and Termination with ROMP

Matthew P. Thompson, Lyndsay M. Randolph, Carrie R. James, Ashley N. Davalos, Michael E. Hahn, and Nathan C. Gianneschi

Department of Chemistry & Biochemistry, University of California, San Diego, La Jolla, CA, U.S.A.. Fax: XX XXXX XXXX; Tel: XX XXXX XXXX

Nathan C. Gianneschi: ngianneschi@ucsd.edu

Abstract

In this paper we compare and contrast three approaches for labelling polymers with functional groups via ring-opening metathesis polymerization (ROMP). We explored the incorporation of functionality via initiation, termination and propagation employing an array of novel initiators, termination agents and monomers. The goal was to allow the generation of selectively labelled and well-defined polymers that would in turn lead to the formation of labelled nanomaterials. Norbornene analogues, prepared as functionalized monomers for ROMP, included fluorescent dyes (rhodamine, fluorescein, EDANS, and coumarin), quenchers (DABCYL), conjugatable moieties (NHS esters, pentafluorophenyl esters), and protected amines. In addition, a set of symmetrical olefins for terminally labelling polymers, and for the generation of initiators *in situ* is described.

Introduction

In the development of labelled polymers, and polymeric nanoparticles, one desires synthetic approaches that allow the most direct route to the incorporation of functional moieties with minimal post-polymerization modifications, and/or post-particle-formation conjugations^{1–17}. The most desirable route is via the direct incorporation of functional groups during the polymerization process itself (i.e. as monomers, initiators or termination agents), preventing the need for subsequent low yielding and difficult to characterize *graft-to* reactions on macromolecules or at particle surfaces. Moreover, post-polymerization modifications and reactions on particle surfaces are difficult to control and yield unpredictably labelled materials. The problem is compounded for particles where chemical functionalities can be difficult to elucidate on nano- and microscale surfaces, and/or exceptionally difficult to reproduce. In our work, we have chosen to focus on a functional group tolerant living polymerization method precisely because of the multiple options available for directly incorporating complex functional groups^{18–21}. The goal is to avoid the need for as many

© The Royal Society of Chemistry

Correspondence to: Nathan C. Gianneschi, ngianneschi@ucsd.edu.

†Electronic Supplementary Information (ESI) available: [Synthetic procedures and characterization are available]. See DOI: 10.1039/b000000x/

reactions performed post-polymerization as possible given the substrate scope of the chosen initiator. Where this is not possible, in the last resort, one desires a polymer or particle decorated with functional groups enabling standard, high yielding conjugation reactions. This is a common goal for those interested in functional nanoparticles capable of expressing some functionality on their shell and/or their core. Therefore, our aim in this paper is to elucidate the capability of ring-opening metathesis polymerization (ROMP) with respect to the incorporation of several classes of functional moiety, representing a range of generally desirable properties. ROMP was chosen as it is an important and useful polymerization method for the generation of well-defined polymers of low polydispersity and highly functionalized architecture^{3, 16, 17, 22}. Multiple initiators are commercially available^{23–26} and can exhibit good stability in ambient conditions making them generally accessible^{25–29}. These properties make ROMP particularly amenable to producing specialized functional polymers for synthetic, biomedical and nanomaterials applications, especially where complex copolymers generated via direct polymerization of functional groups are desirable^{3, 16, 17, 20, 21, 30–34}. There are three opportunities to introduce functionality into polymers via ROMP, (1) the use of an initiator containing a functional alkylidene (Figure 1 - ii), (2) the use of strained olefin-based monomers containing various functionalities (Figure 1 - i, iii), and (3) the use of functionalized termination (or chain transfer) agents (Figure 1 - iv)³⁵. The most popular and easily deployed method for preparing functional polymers is through the use of monomers that either contain the desired functionality or allow for its incorporation *via* a post-polymerization modification^{16, 17, 35}. In addition, the use of functionalized termination agents that allow end-labelling of polymers has garnered increasing attention^{30, 36–43}. By contrast, specially functionalized initiators are underutilized^{5, 26, 44–46}, most likely because changes to the initiator structure can result in changes to the initiation and propagation rates and hence overall polymer quality and predictability in synthesis. Herein, each of these approaches are assessed and utilized for the preparation of micellar nanoparticles assembled from fluorescently labelled amphiphilic block copolymers.

RESULTS AND DISCUSSION

Polymer labelling via ROM/ROMP

Labelling studies were initially conducted by employing the most convenient approach; namely, the incorporation of dye-modified monomers by doping them in small quantities together with nonfunctional monomers. This procedure has been used via ROMP, for introducing small quantities of functional groups into polymers as tags, without dominating polymer structure⁴⁷. To produce end-functionalized polymers, with incorporation of minimal quantities of dye label, we sought to begin polymerization reactions with a 1:1 ratio of monomer to initiator (M:I), followed by addition of a second monomer (in appropriate stoichiometric excess with respect to initiator) for chain extension (Figure 2). We term this procedure, ROM/ROMP, for ring-opening metathesis followed by ROMP. This procedure was planned, as postulated by Sampson and coworkers, as a facile approach to polymer tagging⁴⁷. To examine the viability of this method, norbornene monomers **1** (N-hydroxysuccinimide (NHS) ester) and **2** (a Boc-protected amine) were utilized as they contain functional groups amenable to subsequent conjugation reactions. The first step was

to verify the ability of these monomers to undergo ROMP as determined by ^1H NMR. The disappearance of the norbornene olefin at ~ 6.3 ppm was monitored at various time points after addition of the catalyst (M:I = 20:1). Both monomers **1** and **2** show complete conversion to polymer after 4 minutes (Supporting Information). For the labelling experiment, **1** was mixed with either initiator **I** or **II** and allowed to stir for 20 min to insure complete conversion to the ring opened form (Figure 2, step i). Subsequently, the reaction was quenched by addition of an excess of ethyl vinyl ether (Figure 2 step ii). The ring-opened product corresponding to a single monomer was isolated by column chromatography and characterized by NMR and mass spectrometry (Table 1 entries 1 and 2). The olefin region of the proton NMR shows the presence of multiple isomers consistent with the splitting pattern expected (Supporting Information) and an observed 1:1 ratio of backbone olefin protons to phenyl protons. When norbornene monomer **2** was subjected to the same experimental conditions, similar results were obtained, as shown in Table 1 entries 3 and 4. As an additional confirmation of our characterization of the single ring-opened product, we subjected monomers **1** and **2** to conditions favouring the cross-metathesis reaction. This consisted of 5 mol % initiator **I** or **II** with respect to monomer, and 10 equivalents of styrene. The isolated products gave NMR and mass spectrometry data that are consistent with those obtained for material isolated after quenching a 1:1 reaction of monomer to initiator with ethyl vinyl ether (Supporting Information).

Having successfully demonstrated the ability to generate the single ring-opened species, we next focused on demonstrating that these reaction conditions could be employed to synthesize end-functionalized polymers by ROM/ROMP. Monomers **1** and **2** were again used as test cases for this strategy. A 1:1 reaction mixture of monomer to initiator was employed to generate a living species (Figure 2 - i) followed by the addition of monomer **3** (m equivalents) and subsequent quenching of the polymerization by addition of excess ethyl vinyl ether (Figure 2 steps iii and iv). This procedure gave polymers (e.g. **12** and **16**, Table 2) with low PDI and expected molecular weights as characterized by ^1H -NMR, MALDI-MS (where possible), and size-exclusion chromatography using a multiangle light scattering detector (SEC-MALS). To explore the generality of this tagging approach via ROM/ROMP, we studied norbornene monomers with functionalities generally considered useful in subsequent conjugation reactions, including maleimide (**4**), hydroxylamine precursor (**6**) and protected amine (**11**). Furthermore, several dyes for labelling polymers were used, consisting of coumarin (**5**), DABCYL (**7**), fluorescein (**8**), and EDANS (**9**). Finally, the simple hydrophilic moiety (**10**) was used, which is subsequently useful in micellar nanoparticle formation (*vide infra*). In each case, polymerizable norbornene moieties were used as derived from commercially available *cis*-5-norbornene-*exo*-2,3-dicarboxylic anhydride or 5-norbornene-2-carboxylic acid (resolved prior to use to give *exo*-5-norbornene-2-carboxylic acid)⁴⁸. For ROM/ROMP of each functional monomer, **3** was used as the monomer included for chain extension. Conveniently, ^1H -NMR made it possible to determine the ratio of either the phenyl or benzyl protons from **3** with respect to distinct proton signals for the single ring-opened monomers (unless otherwise noted in Table 2). In this manner, the number of each monomer incorporated could be estimated by applying that ratio to M_w values obtained from SEC-MALS.

Entries A–D in Table 2 show polymers of different length synthesized using NHS monomer **1** as the short label or tag. Due to overlapping signals in the NMR spectra the ratio of NHS to Ph groups could not be obtained. Entries E–I correspond to polymers synthesized using protected amine **2**. Polymers **17–19** (entries F–H) were synthesized from a single reaction mixture by splitting the solution into three equal portions and either terminating the reaction with ethyl vinyl ether (EVE) or adding monomer **2** or **5** followed by EVE. The ratio of monomers incorporated in these systems could be determined using $^1\text{H-NMR}$ by integration of the phenyl or benzyl protons to the protons of the Boc protecting group (for **2**) or one of the aromatic protons of coumarin (for **5**) (See Supplemental Information). Entry I corresponds to a system where we increased the number of equivalents of monomer **3** to generate a larger polymer. Entries J and K correspond to polymers made starting with maleimide **4** using initiator **I** or **II**. Low signal intensity precluded the determination of monomer ratios by NMR for these systems. Entries L–N correspond to polymers synthesized starting with coumarin monomer **5**, with entries M and N being synthesized from a single reaction mixture by splitting the solution into two equal portions and either terminating the reaction with ethyl vinyl ether (EVE) or adding coumarin monomer **5** followed by EVE to give the doubly end-labelled polymer. The ratio of monomers incorporated in these systems was determined using $^1\text{H-NMR}$ by integration of the benzyl protons of **3** to one of the aromatic protons of **5**. In the case of polymer **25** the integral for the benzyl protons was set to the same value as observed in polymer **24**. The change in integration of the coumarin proton signal was then determined to give the number of monomers incorporated at the terminal end of the polymer. Entries O–S corresponds to polymers synthesized starting with hydroxylamine precursor **6** and either initiator **I** or **II**. In all cases doubly end-labelled polymers were synthesized including telechelic systems incorporating conjugatable monomers **1**, **2**, and **6**. The ratio of monomers incorporated in these systems was determined using $^1\text{H-NMR}$. Entry T corresponds to a polymer synthesized starting with DABCYL monomer **7**. The ratio of monomers incorporated in this polymer was determined using $^1\text{H-NMR}$ by integration of the phenyl protons of **3** to one of the aromatic protons of **7**. Finally, entry U corresponds to a polymer synthesized starting with fluorescein monomer **8**. The ratio of monomers incorporated in this polymer was determined using $^1\text{H-NMR}$ by integration of the phenyl protons of **3** to the protons of the pivillac protecting group of **8**.

In addition to the low PDI measured for each polymer, the observed M_w showed expected deviation from theoretically calculated values based on monomer to initiator ratios, within the range commonly observed for ROMP. M_n was measured where possible by MALDI-TOF mass spectrometry and was in good agreement with M_w and M_n determined by SEC-MALS (e.g. Figure 4). The MALDI-TOF spectra also allowed us to assess the effectiveness of this single monomer opening strategy as the incorporation of a single monomer would result in a single mass distribution curve with peak spacing equal to the molecular weight of **3** (253.11 g/mol). The presence of multiple distributions in the spectra with spacing equal to the molecular weight of **5** (282.09 g/mol) indicates the incorporation of more than one functional monomer distributed throughout the population. The number of signals between two adjacent high intensity peaks corresponds to the number of different functional monomers incorporated (Figure 4). As expected the distribution of functional monomers

incorporated in the polymers is dependent on the monomer itself, most likely due to differences in the rate of initiation. The number of incorporated monomers ranges from 1 to 5 with varying distributions depending on the polymer (polymer **23** contains 66% of the singly tagged species) (Supporting information). This combination of data supports the conclusion that it is of course not possible to truly tag each polymer with a single monomer via this method. Rather, it provides a facile method for including close to one equivalent of functional moiety dispersed throughout the population.

Exceptions to the generally well-defined polymers shown in Table 2 were observed for polymers using maleimide monomer **4** as well as dye monomer **7**. These polymerization reactions gave small amounts of high molecular weight products in addition to polymers of the desired molecular weight (see Supporting information). In addition, the higher polydispersities arising from utilizing these monomers in ROM/ROMP is consistent with our observations for corresponding homopolymers of **4** (Supporting information).

The spectrophotometric properties of dye monomers such as **5** were used as a handle for characterizing the degree of incorporation into the population. For example, monitoring the UV absorption at 325 nm allows one to observe the coumarin moiety present in polymers **18**, **23–25**, **27**, and **28**. To utilize this feature in the analysis of end-functionalized polymers, a telechelic polymer containing a protected amine group at one end, and a coumarin moiety at the other (**18**), was synthesized by splitting off an aliquot of **17** prior to quenching, for addition to **5**. The SEC traces showing light scattering (LS), refractive index (RI) (Figure 5A) and UV intensities (Figure 5B) are given for polymers **17** and **18**. The plot of intensity vs. time for light scattering and differential refractive index (Figure 5C) shows similar traces for **17** and **18**, however there is a dramatic increase in the absorption at 325 nm for entry **18** (Figure 5B), consistent with the incorporation of coumarin monomer **5**. Based on M_w values derived from SEC-MALS analysis and UV absorption, the number of coumarin moieties in the polymer could be calculated. For example, using UV absorption at 325 nm for entries G, L–N, P, and Q (Table 2) the number of coumarin moieties incorporated into the polymers was calculated to be 3.60 ± 0.13 , 1.02 ± 0.02 , 1.09 ± 0.08 , 1.81 ± 0.18 , 1.02 , and 1.00 , respectively (Supporting Information).

In addition to the polymerization of coumarin monomer **5** for tagging polymers, we assessed the efficiency of post-polymerization modification of polymers containing NHS ester functionalities. To achieve this polymer **12** was treated with 5 equivalents of 7-hydroxycoumarin and 10 equivalents DIPEA in CH_2Cl_2 for 18 hrs. After purification via repeated precipitations from dichloromethane by addition to cold methanol, the polymer was analyzed by SEC-MALS (Figure 5C). An increase in UV absorption at 325 nm is again noted for the polymer treated with coumarin when compared to the original polymer (Figure 5D). A coupling efficiency of only 13% was obtained using this post-polymerization modification reaction. This highlights the problem with relying on post polymerization modifications to install functionality as rigorous optimization of reaction conditions and or conjugatable groups may be required to obtain a high level of conjugation. In addition to our coumarin studies, protected fluorescein monomer **8** was used to synthesize polymer **32** (Table 2, with the SEC-MALS trace for polymer **32** given in Figure 5E). Deprotection was facilitated by treatment of the polymer with a solution of ammonium hydroxide in DMF.

Upon addition of base, the colour of the solution turned yellow to the eye, signifying the presence of the fluorescein moiety. Fluorescence spectra of **32** before and after deprotection are shown in Figure 5F and indicate a large increase in fluorescence after treatment with base confirming the incorporation of the fluorescein monomer. Using UV absorption at 510 nm, the number of fluorescein units incorporated in polymer **32** was calculated to be 1.11 ± 0.15 (Supporting Information).

Notably, polymer, **32**, demonstrated that labels could be incorporated on the end of the chain in small quantities. Therefore, we next aimed to prepare two polymers that were identical except for the dye used as the end-label. Specifically, we aimed to determine if amphiphilic block copolymers made in this fashion could form labelled micelles incorporating different dyes, but with equivalent morphologies in their final state. This would imply that one could use this tagging strategy to routinely label polymers and particles with different groups, without greatly influencing their overall properties with respect to particle formation. To examine this, we prepared a set of amphiphilic polymers containing either a tag of EDANS or DABCYL (Table 3, Figure 6). A block copolymer of structure, **3₉₁-b-10₆** was prepared, and then split into two equal parts while the polymer was still living. To these two solutions was added one equivalent of **7** or **9**. The resulting polymers **33** and **34** were formulated separately into two particles, **P1** and **P2** via dialysis from DMSO into water⁴⁹. In addition, they were mixed together in a 1:1 ratio in DMSO and slowly transitioned from organic solvent into water to form a fluorescently quenched particle (**P3**). The newly formed micellar aggregates were characterized by dynamic light scattering (DLS) and transmission electron microscopy (TEM) (Table 3, Figure 6). As revealed by TEM, **P1**, **P2**, and **P3** each exhibit a mixed phase of spherical and cylindrical micelles, but were dominated by cylindrical micelles of similar dimensions. The spectral properties of fluorescently labelled aggregates **P1–P3** were analyzed by exciting each of the structures at 335 nm. As shown in Figure 6D, the characteristic EDANS emission maximum is observed at 450 nm for **P1**. However, **P3**, containing both donor (EDANS) and quencher (DABCYL) shows a significant decrease in fluorescence consistent with these dyes now interacting within the Förster radius⁵⁰. Indeed, it can be concluded that the EDANS and DABCYL in **P3** must be within 33 Å of one another⁵¹. Most notably, the consistency in overall morphology is extremely promising with respect to deploying this tagging approach without subsequently perturbing the formation of polymeric nanoparticles.

Polymer labelling via termination of ROMP

While we have successfully shown in the previous section, that a 1:1 ratio of monomer to initiator is effective for incorporating tags of functional monomers on to the ends of polymers, it is desirable to have a more robust approach where one can more reliably incorporate a single functional unit onto each polymer. To facilitate this, we synthesized a number of termination agents (**35–43**) that incorporate dyes, conjugatable groups, and hydrophilic groups (Figure 7). These termination agents (TAs) were synthesized from *cis*-1,4-dichloro-2-butene by nucleophilic substitution reactions (Supporting Information). To develop these novel agents for use by us and others, the efficiency of termination was determined using a ¹H-NMR assay. We postulated that the ¹H-NMR signal corresponding to the alkylidene moiety would be useful for monitoring the termination (cross metathesis)

process (Figure 8). As an initial test of this idea, we chose to evaluate the pentafluorophenol (PFP) termination agent (PFP-TA) **36**. $^1\text{H-NMR}$ spectra were recorded for the free initiator (Figure 8A-i, 8B-i) prior to the addition of monomer **11**, and of the living polymer 20 min after the addition of **11** (Figure 8A-ii, 8B-ii) The living polymer was then split into two pots, with either a large excess of ethyl vinyl ether added to quench the reaction and generate ruthenium species iii (Figure 8A-iii, 8B-iii) or 2 equivalents of **36** added to the reaction to generate species iv (Figure 8A-iv). Spectra were recorded 30 min and 60 min after addition of **36** (Figure 8B-iv). A large excess of ethyl vinyl ether was added to the PFP-TA sample to generate ruthenium species iii (Figure 8A-iii'), and after 20 min a spectrum recorded (Figure 8B-iii'). As shown in Figure 8B, the chemical shift of the alkylidene proton of each species has a distinct chemical shift and could be used to monitor the efficiency of termination. Addition of **36** results in a change in the chemical shift of the alkylidene proton from 18.5 ppm to 19.0 ppm (Figure 8B-ii and 8B-iv respectively). After 60 minutes, complete conversion of living polymer (ii) to terminated polymer (iv) was observed. Addition of ethyl vinyl ether results in the conversion of complex (iv) to (iii') which is obtained directly by addition of ethyl vinyl ether to living polymer ii (Figure 8A-iii). The efficiencies for all terminations agents were determined to be quantitative via this method except for **41** (DABCYL) (Figure 8C). This was attributed to the relatively poor solubility of **41** which begins to precipitate from solution after 30 minutes. Increasing the length of time for termination and changing the solvent to DMF did not increase the efficiency of termination.

As a demonstration of the utility of the tagging with functional termination agents, we synthesized a set of amphiphilic block copolymers end-labelled with dyes and formulated them into micellar nanoparticles. An amphiphilic block copolymer **341-b-1123** was synthesized using initiator **II**, and split into 4 portions while living, followed by termination with **39**, **40**, **41**, or ethyl vinyl ether. Similar to the study performed as described for amphiphilic polymers **33** and **34** generated via the ROM/ROMP process, we chose dye TA combinations known to operate either as a quencher (DABCYL, **41**) or as a FRET acceptor (rhodamine, **40**) of the donor, fluorescein (**39**). Polymers **44-47** were characterized by SEC-MALS (Figure 9A) displaying a major peak at approx. 22 min for all four polymers. Polymers **46** and **47** display a detectable peak due to a higher molecular weight species (shoulder at earlier retention times) prevalent in the light scattering data. We postulate this is due to some aggregation or only due to small quantities of material as the RI signal is weak (Figure 9B) at 20 min retention times in comparison with the major peak observed at 22 min. Indeed, percent by mass characterization by SEC-MALS indicates the peak at 22 min contains >99% of the material with a low polydispersity between 1.01 – 1.09 (Table 4).

To further confirm the incorporation of the dye-labelled termination agents, fluorescence and UV-VIS spectra of polymers **44-47** were taken (Figure 9C-E). The emission spectra of fluorescein were compared to polymer **44** (terminated with EVE) by exciting both polymers **44** and **45** at 470 nm in DMF and monitoring the fluorescence intensity at 563 nm. As shown in Figure 9C, there is no detectable peak at 563 nm for polymer **44** as expected, with a significant increase with fluorescein incorporated. Similarly, **46** was excited at 543 nm and the fluorescence intensity monitored at 592 nm, showing observable fluorescence with rhodamine present, compared to **44**. Lastly, the DABCYL labelled polymer **47**, was

examined via UV spectroscopy and compared to **44**. As expected, no significant absorbance was visible at 444 nm for polymer **44**, however polymer **47** containing the DABCYL TA, shows a characteristic absorbance at 444 nm in DMF (Supporting Information).

Following this initial characterization, dye-labelled block copolymers **44–47** were formulated into particles via slow transition into water by dropwise addition of water to a 1 mg/mL solution of polymer in DMSO followed by dialysis against water⁴⁹. These dye combinations were chosen because fluorescein is a donor for both rhodamine and DABCYL and can be used to study the assembly properties of resulting nanoparticles made up of given ratios of donor to acceptor carrying polymers^{11, 52–59}. Initially, each of the individual polymers were dialyzed from DMSO into water (to generate **P4 – P7**) and were analyzed by DLS and TEM (Figure 10A–D and Table 5). To account for any possible self-quenching (arising from fluorescein), a mixed particle (**P8**) containing the unlabeled **44** and fluorescein-labelled **45** was prepared (Figure 10E). Mixed dye particles **P9** and **P10** were prepared by dialysis by diluting the acceptor into the donor in a co-solvent (DMSO) such that the amount of acceptor was higher than that of the donor (Supporting Information). It was determined by UV spectroscopy that **P9** contained a 1:9 ratio of donor-to-acceptor and **P10** contained a 1:1.5 ratio of fluorescein-to-DABCYL. All particles **P4 – P10** were characterized by TEM and DLS (Table 5 and Figure 10A–G). Each of these particles is spherical in morphology, although some are spherical micelles, while others are larger, and are likely vesicular (e.g. multilamellar vesicles). This set of nanoparticles were then analyzed by fluorescence spectroscopy to characterize the fluorescence properties of the singly labelled particles and mixed nanoparticles. First, a fluorescence emission spectrum was measured for **P5–P7** while exciting at 470 nm to determine if indeed no significant fluorescence intensity was visible without fluorescein (Figure 10H). Figure 10I shows the result of exciting **P8** at 470 nm, exhibiting a characteristic fluorescein maximum intensity emission at 522 nm. In mixed particles **P9** and **P10** a decrease in the overall fluorescein emission intensity is apparent due to the presence of acceptor. A decrease in the fluorescein emission intensity and an increase in rhodamine fluorescence at 569 nm are observed for **P9**, indicating that the donor and acceptor must be within the Förster radius. In the case of **P10**, it illustrates the principle by completely quenching the fluorescein signal by DABCYL, again indicating that the fluorescein and quencher are in communication.

Although we previously have used this type of donor/acceptor interaction in determining the upper limit of the critical aggregation concentration (CAC)⁵⁸, we were unable to do so for these systems as the detection limit of fluorescence is reached before a loss in FRET-signal intensity is observed (Supporting Information). Other common methods used to determine this concentration, including the use of solvchromatic dyes such as pyrene to observe successful micellarization^{60–65} have not yet met with considerable success in our hands for these ROMP-based micelles, possibly due to their high stability.

In addition to determining particle stability, we sought to utilize the direct labelling strategy to elucidate structural features of the particles. The donor–acceptor (D–A) distance distribution was determined by analyzing the time-domain intensity decay of the donor (Figure 11A). Therefore, the data was fit as a summation of donor decays for all accessible D–A distances (Figure 11A). The mean distance between fluorophores, r , was determined

by fluorescence lifetime and plotted as a probability function (Figure 11B–C) for both **P10** and **P11**. For **P10** (particle radius from TEM = 50 nm), the mean distance between donor and acceptor is, $r = 6.57 \pm 0.14$ nm, which was then converted to a decay lifetime $\tau_{DA} = 2.66 \pm 0.23$ ns (Supporting Information). In the case of **P11** (particle radius from TEM = 75 nm), the mean distance between donor and acceptor is, $r = 6.55 \pm 0.08$ nm, and $\tau_{DA} = 2.23 \pm 0.13$ ns. This change in lifetime indicates that the fluorophores are interacting with one another, in positions distributed over the surface of the particles within the Förster radius.

Polymer labelling via initiation of ROMP

As noted in the introduction, the most underutilized strategy for labelling polymers via ROMP has been the use of novel initiators^{5, 26, 44–46}. We take inspiration here from a method demonstrated by Grubbs and co-workers that allows the generation of multiple polymer batches from a single catalyst through a recycling process⁶⁶. The strategy relies on the difference in reactivity between the olefin termination agent and the olefin of the strained norbornene⁶⁷. Initially, the initiator and a chain transfer reagent were stirred together for 20 min to generate the cross-metathesis product (i.e. new functional initiator). Utilizing this approach, addition of a norbornene monomer followed by quenching with ethyl vinyl ether results in polymers with a single functional group installed via the initiator rather than by termination of the reaction (Figure 12). This strategy allows for the single incorporation of two different functional groups at each end of the polymer if a functional TA is used (telechelic polymers). Here, the fluorescein termination agent **39** was used to demonstrate the viability of this method. TA **39** (2 equiv.) was stirred with initiator **II** for 20 minutes followed by addition of monomer **3** (25 equiv.). After 3 minutes the reaction was split in two and quenched with either ethyl vinyl ether or the Boc-protected amine TA **37** (10 equiv.). The latter was quenched with ethyl vinyl ether after 30 minutes to ensure complete termination of the reaction and quenching of the initiator. The polymers were purified by repeated precipitation from cold methanol until pure as indicated by thin-layer chromatography on silica. ¹H NMR of the two resulting polymers shows the presence of both the fluorescein and Boc-amine moieties in addition to the phenyl moiety of monomer **3**. Integration of the *t*-Butyl group for Pivalic protected fluorescein to the phenyl protons of monomer **3** and the, *O-t*-Butyl for the Boc-amine gives a ratio of 1: 30: 0 for the EVE terminated polymer and a ratio of 0.8:30: 1 for Boc-protected amine terminated polymer. The decrease in the number of Pivalic groups compared to the number of phenyl groups demonstrates the limitation of integration as complete monomer conversion was observed before splitting the reaction mixture for termination as this ratio should be constant in both polymers. However, molecular weights determined by SEC-MALS are consistent with the ratio determined by NMR (see supporting information). We conclude that this approach is easily deployed for the end-labelling of polymers via ROMP for monomers that polymerize rapidly as this minimizes the time that the growing polymer is exposed to the still reactive CTA. Indeed, it provides a clean approach for the generation of telechelic systems, and should be useful where synthetic limitations require the incorporation of functional groups at the beginning of polymerizations. This, for example, can occur where a given monomer is insoluble or problematic during polymerization or characterization.

Conclusions

In this paper we have described three approaches for the incorporation of functional groups into polynorbornenes via ROMP. These involve dosing in small quantities of modified norbornene for the polymerization of dyes, the use of modified termination agents for efficient end-labelling, or the use of *in situ* generated initiators. To demonstrate these strategies, we have prepared several new monomers and TAs; both conjugatable and fluorescent. Furthermore, we have formulated a variety of the resulting polymers into labelled nanoparticles. In summary, with an array of strategies in hand for preparing well-defined, labelled polymers, materials can be synthesized that carry a diverse array of functionality. Here we have described this in the context of fluorescence, however, ongoing studies in our laboratories involve the incorporation of peptides, nucleic acids and other types of contrast agents. These studies include investigations of the utility of such systems in targeting/imaging strategies *in vivo*. We contend that it is absolutely critical to the success and progress of relatively complex nanoparticle systems that we have the ability to easily prepare and characterize them. Finally, our goal here was not to conduct an exhaustive, comprehensive study of all possible functional groups of interest, but rather to demonstrate and contrast easily utilized approaches to achieving polymer labelling via ROMP.

Supplementary Material

Refer to Web version on PubMed Central for supplementary material.

Acknowledgments

The authors acknowledge support for this program from AFOSR through a PECASE (FA9550-11-1-0105) and a BRI grant (FA9550-12-1-0435). In addition, we acknowledge support from ARO (W911NF-11-1-0264). Furthermore, we thank NIH (NIBIB) for their generous support (1R01EB011633) and via a NIH Director's New Innovator Award (1DP2OD008724). N.C.G. acknowledges the Henry & Camille Dreyfus Foundation for a New Faculty Award.

Notes and references

1. Aoshima S, Kanaoka S. Chemical Reviews. 2009; 109:5245–5287. [PubMed: 19803510]
2. Beija M, Charreyre MT, Martinho JMG. Progress in Polymer Science. 2011; 36:568–602.
3. Bielawski CW, Grubbs RH. Prog Polym Sci. 2007; 32:1–29.
4. Broyer RM, Grover GN, Maynard HD. Chem Commun. 2011; 47:2212–2226.
5. Castle TC, Hutchings LR, Khosravi E. Macromolecules. 2004; 37:2035–2040.
6. Guo R, Wang X, Guo C, Dong A, Zhang J. Macromolecular Chemistry and Physics. 2012; 213:1851–1862.
7. Lele BS, Murata H, Matyjaszewski K, Russell AJ. Biomacromolecules. 2005; 6:3380–3387. [PubMed: 16283769]
8. Li M, Li H, De P, Sumerlin BS. Macromolecular Rapid Communications. 2011; 32:354–359. [PubMed: 21433183]
9. Moad G, Rizzardo E, Thang SH. Australian Journal of Chemistry. 2012; 65:985–1076.
10. Nicolas J, Mantovani G, Haddleton DM. Macromolecular Rapid Communications. 2007; 28:1083–1111.
11. Prazeres TJV, Beija M, Charreyre MT, Farinha JPS, Martinho JMG. Polymer. 2010; 51:355–367.
12. Schaefer M, Hanik N, Kilbinger AFM. Macromolecules. 2012; 45:6807–6818.

13. Siegwart DJ, Oh JK, Matyjaszewski K. *Progress in Polymer Science*. 2012; 37:18–37. [PubMed: 23525884]
14. Sumerlin BS. *ACS Macro Letters*. 2011; 1:141–145.
15. Tasdelen MA, Kahveci MU, Yagci Y. *Progress in Polymer Science*. 2011; 36:455–567.
16. Leitgeb A, Wappel J, Slugovc C. *Polymer*. 2010; 51:2927–2946.
17. Slugovc C. *Macromol Rapid Commun*. 2004; 25:1283–1297.
18. Scholl M, Ding S, Lee CW, Grubbs RH. *Organic Letters*. 1999; 1:953–956. [PubMed: 10823227]
19. Trnka TM, Grubbs RH. *Accounts of Chemical Research*. 2000; 34:18–29. [PubMed: 11170353]
20. Hahn ME, Randolph LM, Adamiak L, Thompson MP, Gianneschi NC. *Chem Commun*. 2013; 49:2873–2875.
21. Kammeyer JK, Blum AP, Adamiak L, Hahn ME, Gianneschi NC. *Polymer Chemistry*. 2013; 4:3929–3933. [PubMed: 24015154]
22. Grubbs RH. *Tetrahedron*. 2004; 60:7117–7140.
23. Harrity JPA, La DS, Cefalo DR, Visser MS, Hoveyda AH. *Journal of the American Chemical Society*. 1998; 120:2343–2351.
24. Schrock RR, Murdzek JS, Bazan GC, Robbins J, DiMare M, O'Regan M. *Journal of the American Chemical Society*. 1990; 112:3875–3886.
25. Schwab P, France MB, Ziller JW, Grubbs RH. *Angewandte Chemie International Edition*. 1995; 34:2039–2041.
26. Schwab P, Grubbs RH, Ziller JW. *Journal of the American Chemical Society*. 1996; 118:100–110.
27. Frenzel U, Nuyken O. *Journal of Polymer Science Part A: Polymer Chemistry*. 2002; 40:2895–2916.
28. Sanford MS, Love JA, Grubbs RH. *Organometallics*. 2001; 20:5314–5318.
29. Sanford MS, Love JA, Grubbs RH. *Journal of the American Chemical Society*. 2001; 123:6543–6554. [PubMed: 11439041]
30. Hilf S, Kilbinger AFM. *Nat Chem*. 2009; 1:537–546. [PubMed: 21378934]
31. Khosravi, E.; Castle, TC.; Kujawa, M.; Leejarkpai, J.; Hutchings, LR.; Hine, PJ. *New Smart Materials via Metal Mediated Macromolecular Engineering*. Khosravi, E.; Yagci, Y.; Saveliev, Y., editors. Springer; Netherlands: 2009. p. 223-236.
32. Kiessling, LL.; Mangold, SL. *Polymer Science: A Comprehensive Reference*. Krzysztof, M., Editors-in-Chief; Martin, M., editors. Elsevier; Amsterdam: 2012. p. 695-717.
33. Nomura K, Abdellatif MM. *Polymer*. 2010; 51:1861–1881.
34. Smith D, Pentzer EB, Nguyen ST. *Polymer Reviews*. 2007; 47:419–459.
35. Kilbinger, AFM. *Functional Polymers by Post-Polymerization Modification*. Wiley-VCH Verlag GmbH & Co; KGaA: 2012. p. 153-171.
36. Madkour AE, Koch AHR, Lienkamp K, Tew GN. *Macromolecules*. 2010; 43:4557–4561. [PubMed: 21499549]
37. Chen B, Metera K, Sleiman HF. *Macromolecules*. 2005; 38:1084–1090.
38. Kolonko EM, Kiessling LL. *Journal of the American Chemical Society*. 2008; 130:5626–5627. [PubMed: 18393495]
39. Mangold SL, Carpenter RT, Kiessling LL. *Organic Letters*. 2008; 10:2997–3000. [PubMed: 18563907]
40. Matson JB, Grubbs RH. *Macromolecules*. 2010; 43:213–221. [PubMed: 20871800]
41. Owen RM, Gestwicki JE, Young T, Kiessling LL. *Organic Letters*. 2002; 4:2293–2296. [PubMed: 12098230]
42. Chien M-P, Thompson MP, Barback CV, Ku T-H, Hall DJ, Gianneschi NC. *Advanced Materials*. 2013:n/a–n/a.
43. Rush AM, Thompson MP, Tatro ET, Gianneschi NC. *ACS Nano*. 2013; 7:1379–1387. [PubMed: 23379679]
44. Ambade AV, Burd C, Higley MN, Nair KP, Weck M. *Chemistry – A European Journal*. 2009; 15:11904–11911.

45. Burtscher D, Saf R, Slugovc C. *Journal of Polymer Science Part A: Polymer Chemistry*. 2006; 44:6136–6145.
46. Ambade AV, Yang SK, Weck M. *Angew Chem Int Edit*. 2009; 48:2894–2898.
47. Roberts KS, Sampson NS. *Organic Letters*. 2004; 6:3253–3255. [PubMed: 15355025]
48. Pontrello JK, Allen MJ, Underbakke ES, Kiessling LL. *Journal of the American Chemical Society*. 2005; 127:14536–14537. [PubMed: 16231882]
49. Zhang L, Eisenberg A. *Polymers for Advanced Technologies*. 1998; 9:677–699.
50. Förster T. *Annalen der Physik*. 1948; 437:55–75.
51. Matayoshi ED, Wang GT, Krafft GA, Erickson J. *Science*. 1990; 247:954–958. [PubMed: 2106161]
52. Clegg, RM. *Methods in Enzymology*. David, JED.; Lilley, MJ., editors. Vol. 211. Academic Press; 1992. p. 353-388.
53. Stryer L. *Annual Review of Biochemistry*. 1978; 47:819–846.
54. Lakowicz, JR. *Principles of Fluorescence Spectroscopy*. Springer Science+Business Media, LLC; 1983.
55. Selvin PR. *Nat Struct Mol Biol*. 2000; 7:730–734.
56. Farinha JPS, Martinho JMG. *The Journal of Physical Chemistry C*. 2008; 112:10591–10601.
57. Schillén K, Yekta A, Ni S, Farinha JPS, Winnik MA. *The Journal of Physical Chemistry B*. 1999; 103:9090–9103.
58. Chien MP, Thompson MP, Lin EC, Gianneschi NC. *Chemical Science*. 2012; 3:2690–2694. [PubMed: 23585924]
59. Farinha JPS, Schillén K, Winnik MA. *The Journal of Physical Chemistry B*. 1999; 103:2487–2495.
60. Acharya KR, Bhattacharyya SC, Moulik SP. *Journal of Photochemistry and Photobiology A: Chemistry*. 1999; 122:47–52.
61. Hait SK, Majhi PR, Blume A, Moulik SP. *The Journal of Physical Chemistry B*. 2003; 107:3650–3658.
62. Majhi PR, Mukherjee K, Moulik SP, Sen S, Sahu NP. *Langmuir*. 1999; 15:6624–6630.
63. Turro NJ, Kuo PL. *Langmuir*. 1985; 1:170–172.
64. Kalyanasundaram K, Thomas JK. *Journal of the American Chemical Society*. 1977; 99:2039–2044.
65. Aguiar J, Carpena P, Molina-Bolívar JA, Carnero Ruiz C. *Journal of Colloid and Interface Science*. 2003; 258:116–122.
66. Matson JB, Virgil SC, Grubbs RH. *Journal of the American Chemical Society*. 2009; 131:3355–3362. [PubMed: 19215131]
67. Hanik N, Kilbinger AFM. *Journal of Polymer Science Part A: Polymer Chemistry*. 2013; 51:4183–4190.

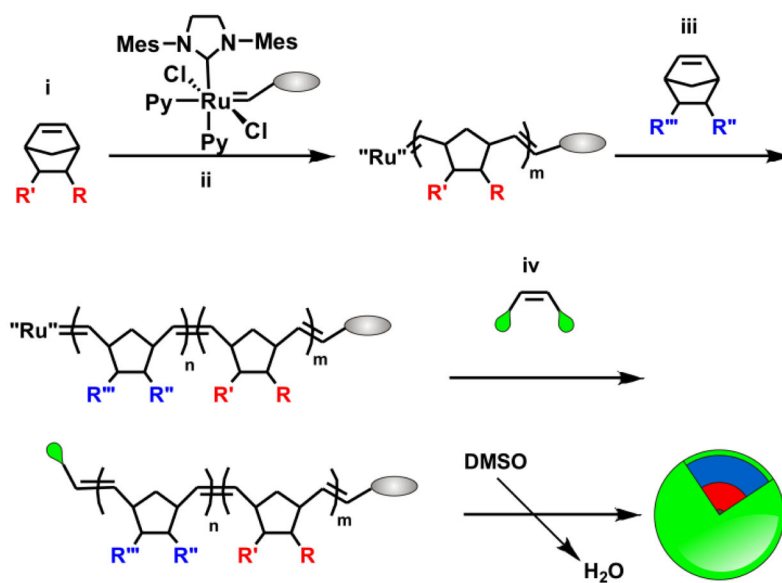
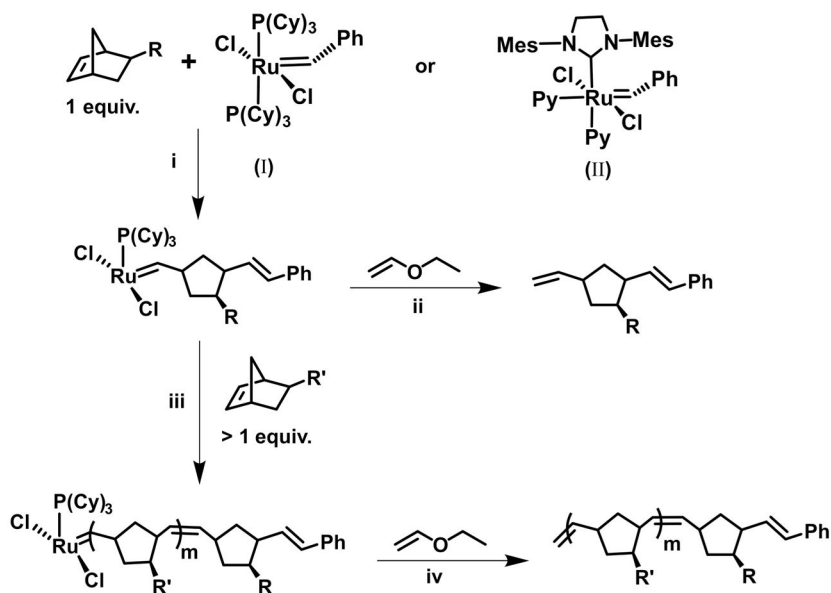


Fig. 1. General scheme for the synthesis of functionalized polymers via ROMP. Monomers (i, iii), initiators (ii) and termination agents (iv) containing functional groups can be used to synthesize labeled amphiphilic polymers that assemble into labeled micelles.

**Fig. 2.**

General scheme for end-functionalized polymer synthesis via ROM/ROMP. (i) One equivalent of monomer is added to the Ru(IV) initiator. (ii) The ring-opened product is isolable following addition of ethyl vinyl ether. (iii) End-functionalized polymers result from the addition of *m* equivalents of a second monomer, followed by termination with ethyl vinyl ether (iv).

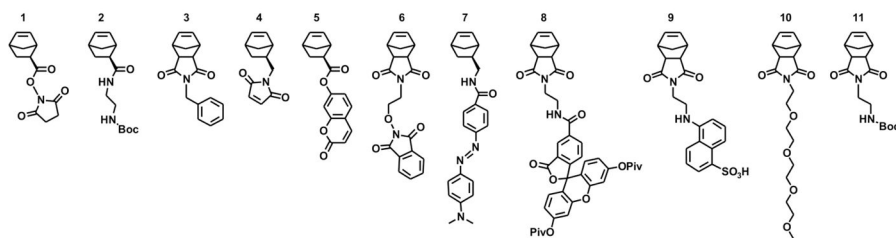


Fig. 3.
Structures of norbornene-based monomers used in this study.

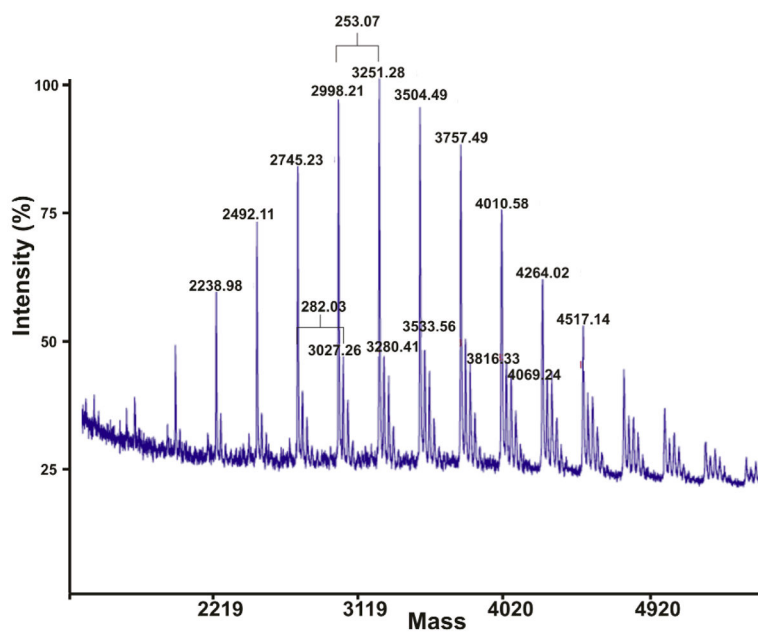


Fig. 4. MALDI MS of polymer **23** showing the polydispersity and revealing the efficiency of the single monomer tagging strategy (**3**, $M_w = 253.11$ g/mol, **5** $M_w = 282.09$ g/mol).

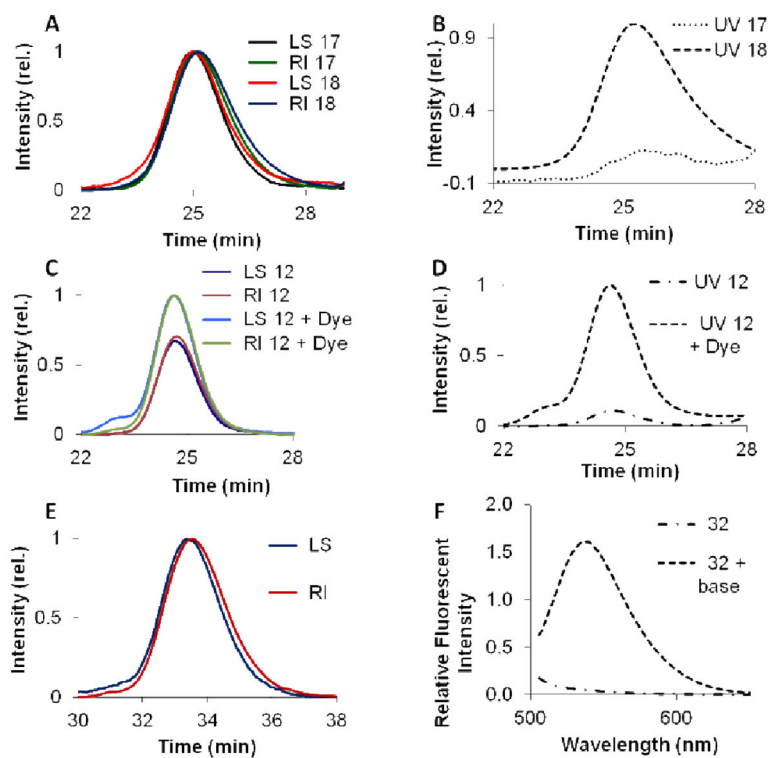


Fig. 5.

SEC traces and fluorescence spectra for polymers **17**, **18**, **12**, and **32**. (A) SEC with scattering intensity and refractive index for **17** and **18**. (B) SEC with UV absorbance for **17** and **18**. (C) SEC with scattering intensity and refractive index for **12** and **12** + 7-hydroxycoumarin. (D) UV traces of polymer **12** before and after conjugation with 4-hydroxycoumarin. (E) SEC-MALS of polymer **32** and (F) fluorescence spectra of polymer **32** before and after removal of the pivillac protecting groups by treatment with base.

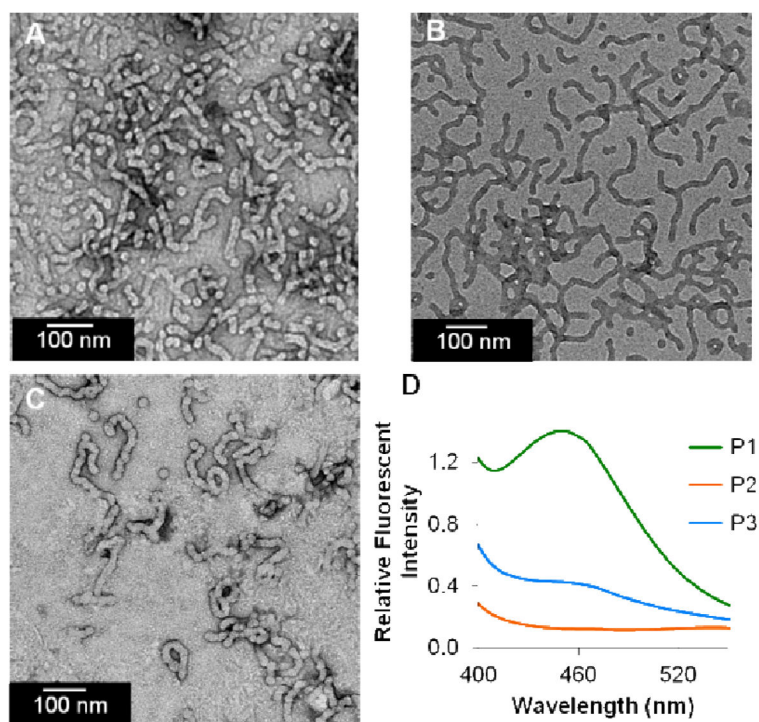


Fig. 6. Transmission electron micrographs (TEM) and fluorescent spectra of **P1**, **P2**, and **P3**. A) TEM of **P1**, B) TEM of **P2**, C) TEM of **P3**, (1% uranyl acetate stain) and D) Fluorescent emission spectrum of **P1** (54.9 μM), **P2** (12.5 μM), and **P3** (54.9 μM EDANS, 12.5 μM DABCYL) with an excitation of 335 nm.

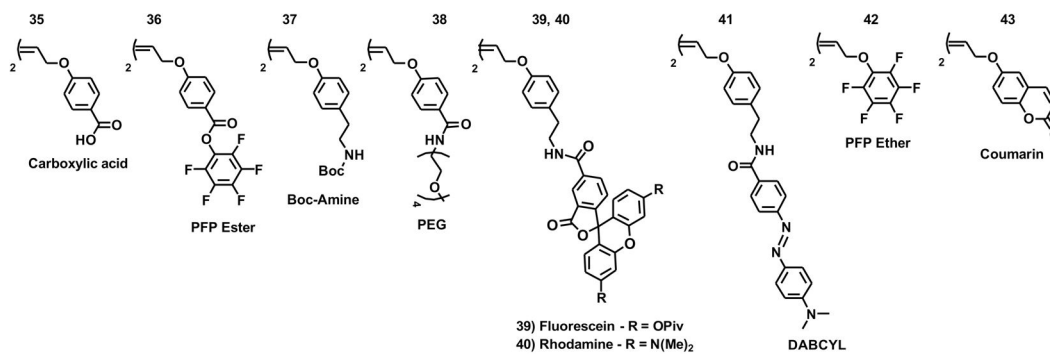


Fig. 7.
Structures of the symmetrical termination agents (TA) synthesized.

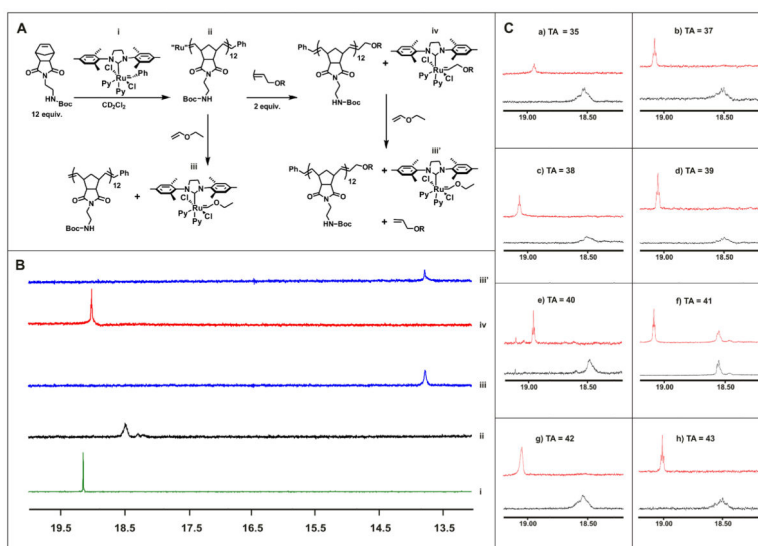


Fig. 8. Termination agent efficiency for **35–43**. A) Scheme outlining termination agent efficiency experiment. B) ^1H NMR spectra of the alkylidene proton of the molecules shown in A for TA **36**. i) Catalyst, ii) Living polymer, iii) Terminated catalyst with ethyl vinyl ether, iv) catalyst terminated with functional termination agent, iii') After quenching the reaction with ethyl vinyl ether. c) ^1H NMR spectra of the alkylidene proton on polymers treated with TAs **35–43**. Bottom (black) spectra corresponds to the living polymer, Top spectra (red) corresponds to polymers after termination with TA's **35–43**.

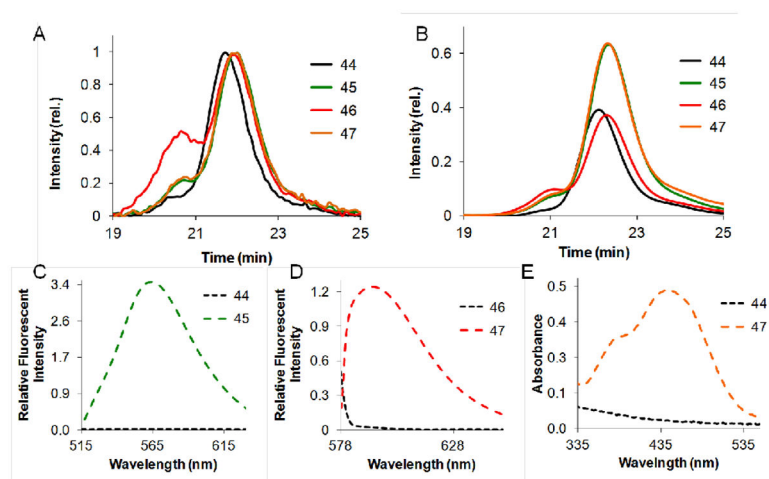


Fig. 9. SEC and spectral characterization for polymers **44–47**. A) SEC trace and scattering intensity of polymers **44–47**. B) SEC trace and refractive index for polymers **44–47**. C) Fluorescent emission spectra of polymers **44** and **45** with an excitation of 470 nm. D) Fluorescent emission spectra of polymers **45** and **47** with an excitation of 543 nm. E) UV-VIS of polymers **44** and **47**.

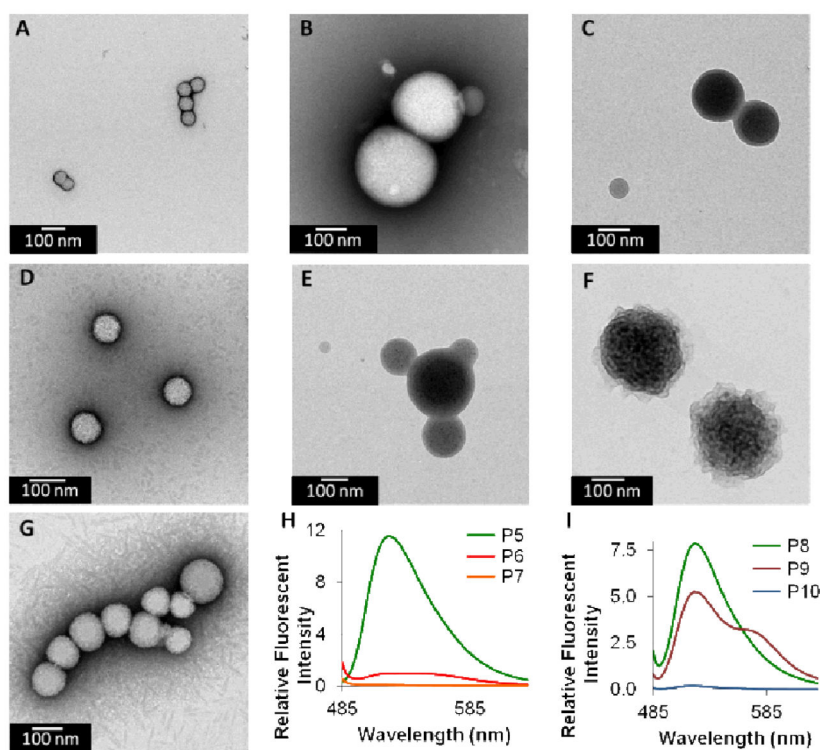


Fig. 10. TEM and fluorescent data of nanoparticles made of A) **P4**, B) **P5**, C) **P6**, D) **P7**, E) **P8** F) **P9**, G) **P10** (1% uranyl acetate stain), H) fluorescence emission spectra of **P5** (4.15 μM), **P6** (36.7 μM), and **P7** (6.19 μM), $\lambda_{\text{ex}} = 470$ nm, and I) fluorescence emission spectra of **P8** (4.15 μM), **P9** (4.15 μM fluorescein, 37.7 μM rhodamine), and **P10** (4.15 μM fluorescein, 37.7 μM DABCYL), $\lambda_{\text{ex}} = 470$ nm

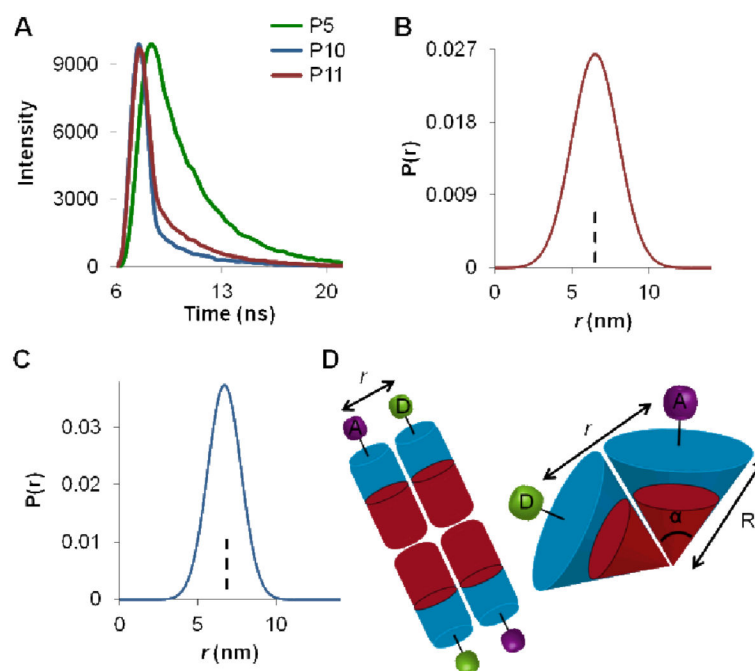
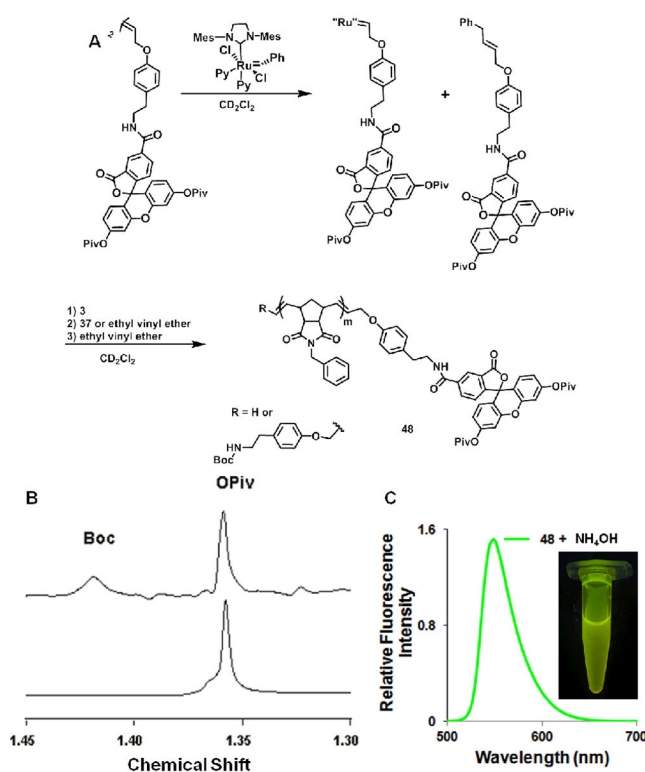
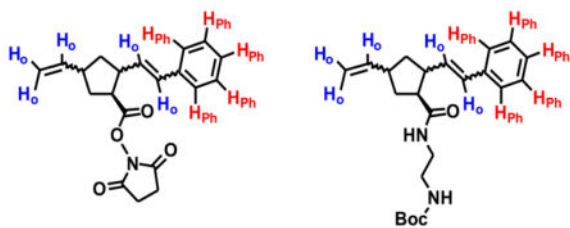


Fig. 11.

Time-domain fluorescence lifetime analysis of **P10** and **P11** and distance distribution of dyes on nanoparticle surfaces. (A) Fluorescence lifetime of **P5**, **P10**, and **P11** giving $\tau_D = 3.01 \pm 0.22$ ns for unquenched fluorescein, **P5**. (B–C) A range of distances, determined from lifetime data, between donor and acceptor in **P10** and **P11** are plotted and expressed as a probability function $P(r)$. (B) The mean distance between fluorescein and rhodamine in **P11**, $r = 6.55 \pm 0.08$ nm with decay lifetime $\tau_{DA} = 2.23 \pm 0.13$ ns. (C) The mean distance between fluorescein and DABCYL in **P10**, $r = 6.57 \pm 0.14$ nm, giving $\tau_{DA} = 2.66 \pm 0.23$ ns. (D) Postulated schematic of the relationship in space between donor and acceptor (r) for a bilayer (vesicular/multilamellar) or spherical arrangement left and right respectively.

**Fig. 12.**

A) Synthesis of telechelic polymer **48** via in situ generation of a functional initiator using TA **39**. B) NMR data: Top spectra, polymer after purification showing signals corresponding to both functional groups. Bottom spectra, polymer quenched with ethyl vinyl ether in step 2. C) Fluorescence data of polymer **48** in DMF after treatment with NH_4OH to remove the protecting groups.

Table 1Results for the single opening of monomers **1** and **2**

| Entry | Mon | Initiator | Mass | H _o /H _{Ph} |
|-------|----------|-----------|--|---------------------------------|
| 1 | 1 | I | 357.00 [M+NH ₄] ⁺ | 1.18 |
| 2 | 1 | II | 356.93 [M+NH ₄] ⁺ | 0.9 |
| 3 | 2 | I | 384.93 [M+H] ⁺ | 0.9 |
| 4 | 2 | II | 384.81 [M+H] ⁺ | 1.05 |

Terminally functionalized polymers synthesized by ROM/ROMP of combinations of three different monomers indicated here as “Mon₁” with “Mon₂”, and/or “Mon₃”.

Table 2

| Entry | Polymer | Initiator | Mon ₁ (ratio to initiator) | Mon ₂ (ratio to initiator) | Mon ₃ (ratio to initiator) | Ratio by ¹ H NMR (Mon ₁ : Mon ₂ : Mon ₃) ^{a,b} | Theoret. M _n (g/mol) | Obs. M _w (g/mol) ^c | Obs. M _n (g/mol) ^d | PDI ^c | % Area ^e | % Yield ^f |
|-------|---------|-----------|---|---|---|--|---------------------------------|--|--|------------------|---------------------|----------------------|
| A | 12 | II | 1 (1:1) | 3 (20:1) | - | nd | 5417 | 6353 | - | 1.01 | 100 | 84 |
| B | 13 | II | 1 (1:1) | 3 (40:1) | - | nd | 10497 | 11440 | - | 1.00 | 100 | 99 |
| C | 14 | II | 1 (1:1) | 3 (60:1) | - | nd | 15577 | 18020 | - | 1.00 | 100 | 90 |
| D | 15 | II | 1 (1:1) | 3 (6:1) | - | nd | 1861 | 2310 | - | 1.04 | 100 | 71 |
| E | 16 | II | 2 (1:1) | 3 (10:1) | - | (1.0: 16.0: 0) | 2921 | 3750 | 4268 | 1.02 | 100 | 67 |
| F | 17 | I | 2 (1:1) | 3 (10:1) | - | (1.0: 12.0: 0) | 2921 | 4838 | 4516 | 1.04 | 99 | 75 |
| G | 18 | I | 2 (1:1) | 3 (10:1) | 5 (1:1) | (1.0: 12.0: 2.3) | 3203 | 5734 | - | 1.06 | 99 | 95 |
| H | 19 | I | 2 (1:1) | 3 (10:1) | 2 (1:1) | (1.0: 12.0: 1.2) | 3201 | 4961 | - | 1.04 | 99 | 70 |
| I | 20 | I | 2 (1:1) | 3 (30:1) | - | (1.0: 36.0) | 7960 | 9571 | - | 1.04 | 100 | 76 |
| J | 21 | I | 4 (1:1) | 3 (10:1) | - | nd | 2844 | 6127 | 4265 | 1.14 | 97 | 88 |
| K | 22 | II | 4 (1:1) | 3 (10:1) | - | nd | 2844 | 6884 | - | 1.02 | 75 | 88 |
| L | 23 | II | 5 (1:1) | 3 (10:1) | - | (1.2: 11.0) | 2923 | 3133 | 3251 | 1.04 | 100 | 83 |
| M | 24 | II | 5 (1:1) | 3 (15:1) | - | (1.0: 11.0) | 4192 | 4000 | 4264 | 1.02 | 100 | 75 |
| N | 25 | II | 5 (1:1) | 3 (15:1) | 5 (1:1) | (1.0: 11.0: 2.7) | 4475 | 4100 | 4517 | 1.08 | 100 | 85 |
| O | 26 | I | 6 (1:1) | 3 (30:1) | 1 (1:1) | (n.d.:38: 0.7) | 8268 | 9906 | - | 1.10 | 100 | 74 |
| P | 27 | I | 6 (1:1) | 3 (25:1) | 5 (1:1) | n.d. | 7049 | 10320 | - | 1.09 | 97 | 99 |
| Q | 28 | II | 6 (1:1) | 3 (25:1) | 5 (1:1) | (n.d.: 25: 1) | 7049 | 6875 | - | 1.01 | 100 | 97 |
| R | 29 | I | 6 (1:1) | 3 (25:1) | 6 (1:1) | (n.d.: 8.0: 1.0) | 7120 | 7850 | - | 1.07 | 95 | 82 |
| S | 30 | II | 6 (1:1) | 3 (25:1) | 6 (1:1) | (n.d.: 22: 1.0) | 7119 | 6309 | - | 1.00 | 100 | 90 |
| T | 31 | II | 7 (1:1) | 3 (10:1) | - | (1.0: 13.0) | 3015 | 2770 | - | 1.05 | 71 | 72 |
| U | 32 | II | 8 (1:1) | 3 (20:1) | - | (1.0: 24.0) | 5915 | 5715 | 5023 | 1.04 | 100 | 74 |

^a Determined from the ratio of Mon₁ to Mon₂ protons, Mon₃ to Mon₂ protons or Mon₁ to Mon₃ protons.

^b Delay time increased to 10 sec to ensure complete relaxation.

^c Determined by SEC-MALS.

^d Determined by MALDI mass spectrometry where possible.

^e Area of largest peak in SEC-MALS trace.

^f Isolated yield. (n.d. = not determinable).

Table 3

Summary of EDANS and DABCYL labelled ROMP polymers and particle characterization.

| Polymer (Particle) ^a | Mon ₁ (DP) ^b | Mon ₂ (DP) ^b | Mon ₃ (DP) ^b | M _n (g/mol) | M _w /M _n | D _h ^c (nm) | PDI ^d |
|---------------------------------|------------------------------------|------------------------------------|------------------------------------|------------------------|--------------------------------|----------------------------------|------------------|
| 33 (P1) | 3 (91) | 10 (6) | 9 (2) | 10540 | 1.038 | 255 | 0.308 |
| 34 (P2) | 3 (91) | 10 (6) | 7 (4) | 10480 | 1.103 | 164 | 0.265 |
| 33 + 34 (P3) | ^e | - | - | - | - | 295 | 0.285 |

^a Subsequent particles formed from amphiphilic polymer **33**, **34**, or **33 + 34** is shown in parenthesis (i.e. P#).

^b Degree of polymerization (DP) of Mon_x.

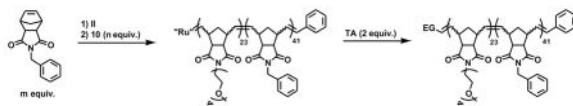
^c Hydrodynamic diameter D_h (uncorrected) of micelles formed from polymers **33**, **34**, or **33 + 34** as determined by dynamic light scattering (DLS).

^d Polydispersity (PDI) as determined by DLS.

^e See polymers **33** and **34** for polymer characterization.

Table 4

Summary of end-group (EG) functionalized polymers synthesized by ROMP of **3** with **10** and terminated with TAs **39–41**



| Polymer | TA | Degree of polymerization of 3 and 13 in the polymer as determined by SEC-MALS | M_n (g/mol) ^b | M_w/M_n ^{b,c} |
|-----------|------------------|---|----------------------------|--------------------------|
| 44 | EVE ^a | 41, 23 | 18460 | 1.01 |
| 45 | 39 | 41, 23 | 18730 | 1.03 |
| 46 | 40 | 41, 23 | 21550 | 1.09 |
| 47 | 41 | 41, 23 | 18660 | 1.04 |

^a Polymer terminated with ethyl vinyl ether (EVE).

^b Determined by SEC-MALS.

^c Determined from the low molecular weight species only (< 99% of sample).

Table 5Summary of particles synthesized from polymers **44–47**

| Particle | Composition ^a | EG(s) ^b | D _h ^c (nm) | PDI ^d |
|------------------------|--------------------------|------------------------|----------------------------------|------------------|
| P4 | 44 | EVE | 146.6 | 0.02489 |
| P5 | 45 | Fluorescein | 314.4 | 0.01418 |
| P6 | 46 | Rhodamine | 312.6 | 0.05280 |
| P7 | 47 | DABCYL | 111.5 | 0.08099 |
| P8 | 44 + 45 | EVE, Fluorescein | 442.1 | 0.01482 |
| p9^e | 45 + 46 | Fluorescein, Rhodamine | 498.8 | 0.02155 |
| P10 | 45 + 47 | Fluorescein, DABCYL | 204.2 | 0.03774 |
| P11^f | 45 + 46 | Fluorescein, Rhodamine | 450.3 | 0.1109 |

^aPolymer(s) used in the formulation of the particles **P4–P11**.

^bEnd group of the polymer after termination.

^cHydrodynamic diameter (uncorrected) as determined by DLS.

^dPolydispersity index (PDI) as determined by DLS.

^eParticle used for CMC measurements.

^fParticle used for fluorescence lifetime measurements.